

## Supporting Information

### **Plasmonic hydrogels for capture, detection and removal of organic pollutants**

*Irene Vassalini\**, *Giovanni Ribaldo*, *Alessandra Gianoncelli*, *Maria F. Casula*, *Ivano Alessandri\**

**SI 1.** Mass spectrum of the  $\beta$ CD-MB binding experiment

**SI 2.** High magnification TEM images of the organic coating around Ag@ $\beta$ CD NPs

**SI 3.** Ag@ $\beta$ CD NPs-alginate bubbles stability at different pH

**SI 4.** Release of AgNPs from Ag@ $\beta$ CD NPs-alginate bubbles

**SI 5.** Release of entrapped MB from Ag@ $\beta$ CD NPs-alginate bubbles

**SI 6.** Characterization of non-functionalized Ag NPs systems

**SI 7.** Comparison between the Raman spectra obtained using as absorbing and SERS substrate

Ag@ $\beta$ CD NPs-alginate bubbles (black) and non-functionalized Ag NPs-alginate

**SI 8.** Intra-bubble Raman intensity variability

**SI 9.** Inter-bubble Raman intensity variability

**SI 10.** Photochemical stability of MB adsorbed on Ag@ $\beta$ CD NPs-alginate bubbles under UV and visible illumination

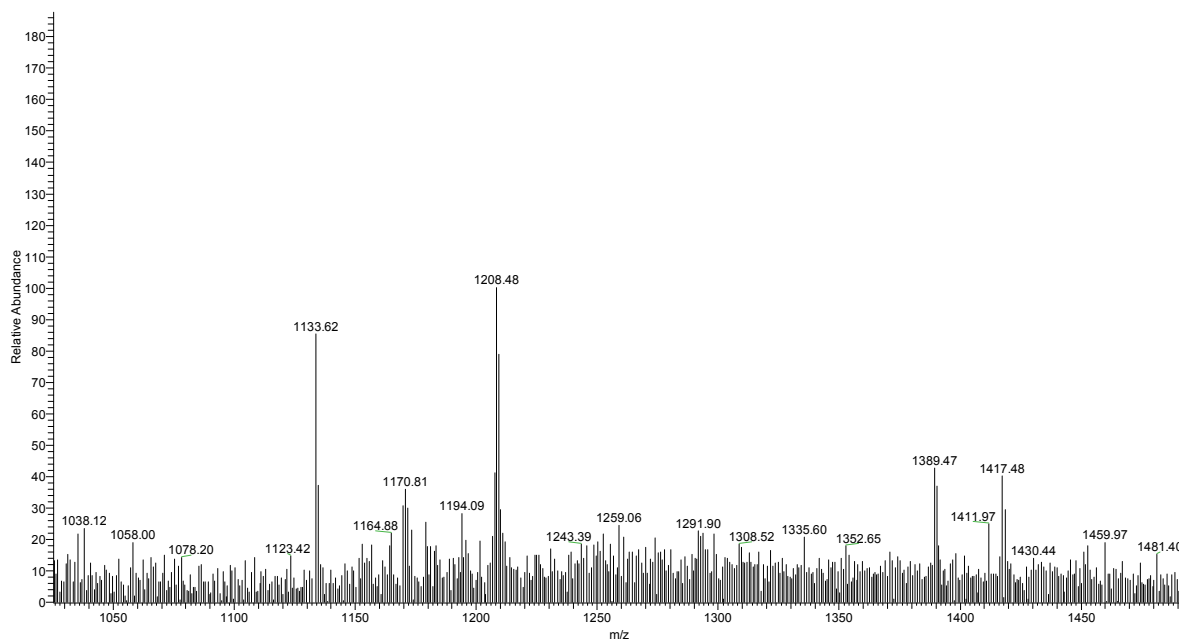


**Figure S1.** Mass spectrum of the  $\beta$ CD-MB binding experiment. The peak at  $m/z = 1333.62$  corresponds to unbound  $\beta$ CD and the peak at  $m/z = 1417.48$  to the  $\beta$ CD-MB complex. The peaks at  $m/z = 1170.81$  and  $1208.48$  are due to  $\text{Cl}^-$  adducts. The peak at  $m/z = 1389.47$  was not identified.

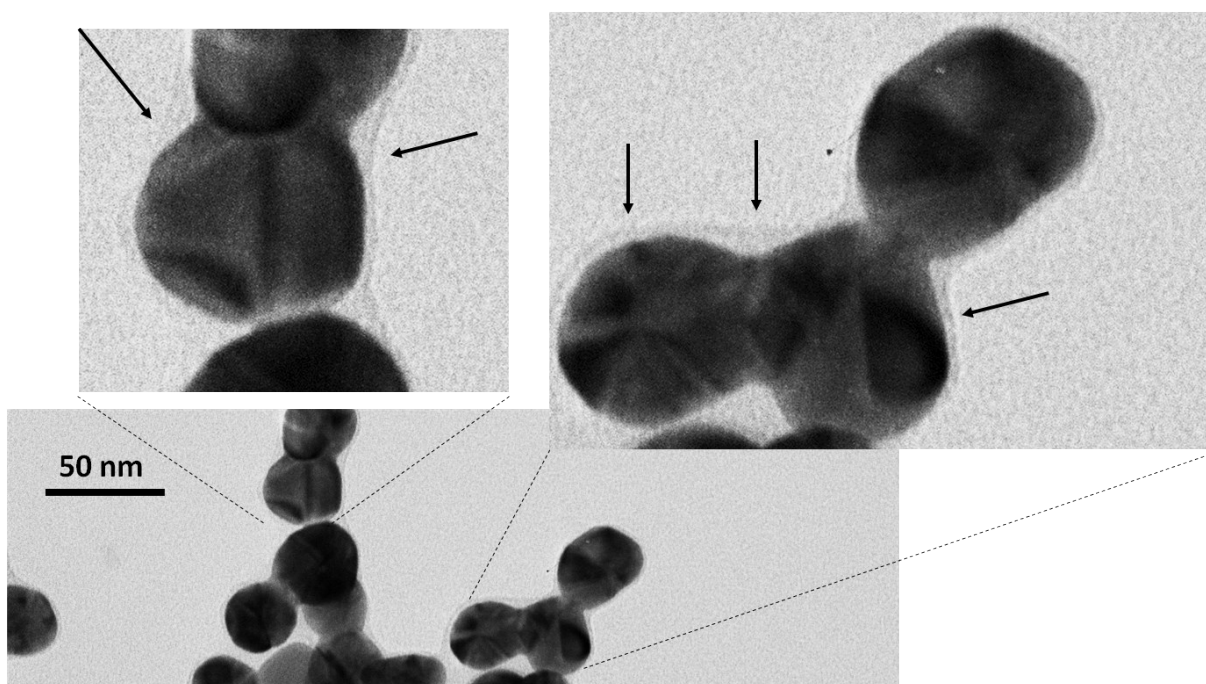


**Figure S2.** High magnification TEM images of  $\text{Ag}@ \beta$ CD NPs synthesized using  $\beta$ CD both as reducing and capping agent. Arrows point to the organic coating.

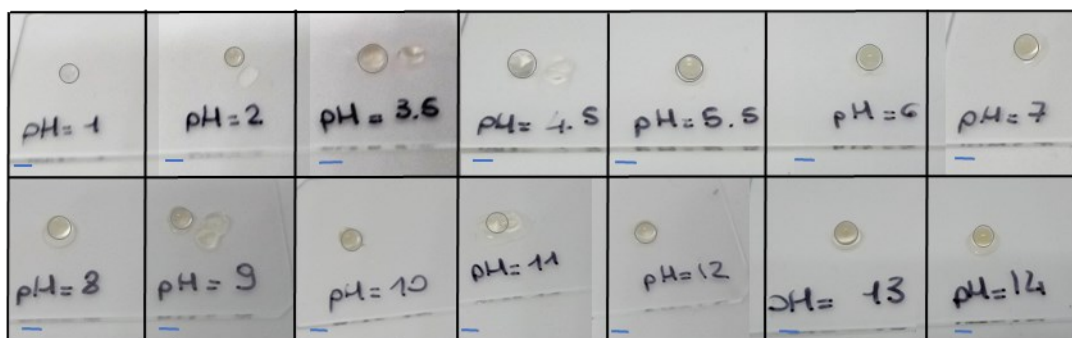


**Figure S3.** Ag@ $\beta$ CD NPs-alginate bubbles stability at different pH of water solution in which are suspended. Blu bar 2 mm.

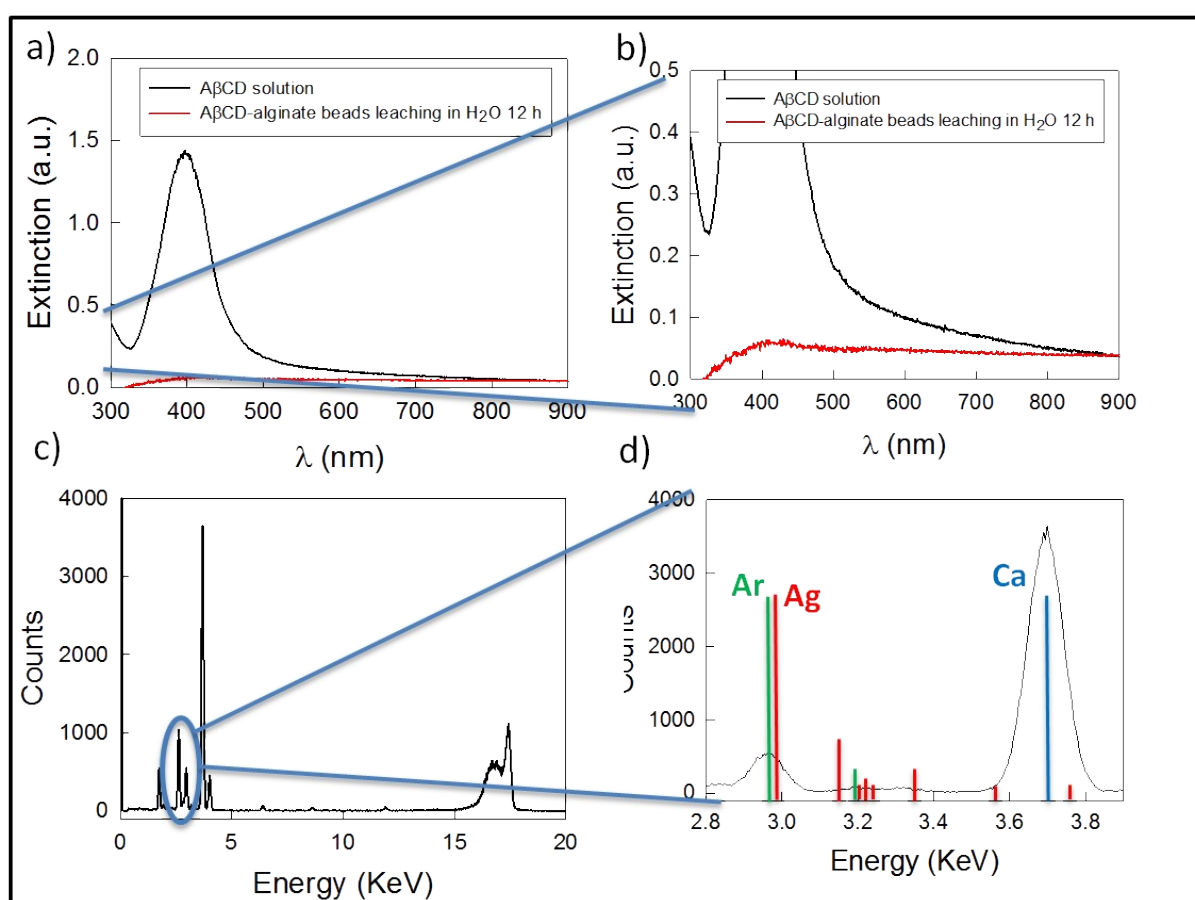


**Figure S4.** a) UV-Vis extinction spectra of an aqueous solution of Ag@ $\beta$ CD NPs before their encapsulation in alginate beads. The localized SPR peak (LSPR) centred at 404 nm, which dominates the spectrum of non-encapsulated samples (black spectrum), indicates the presence of silver nanoparticles in solution. On the other hand, the spectrum acquired from water in which the Ag@ $\beta$ CD NPs-alginate bubbles have been soaked for 12 h does not show any significant contribution from silver (see also a magnification of the LSPR spectral region reported in Figure S4 b); c) In order to reveal the possible presence of silver released from the Ag@ $\beta$ CD NPs-alginate bubbles, total-x-ray-fluorescence (TXRF) analyses were carried out (Figure c). No significant evidence of the presence of silver was detected (see also the zoomed image in Figure S4 d).

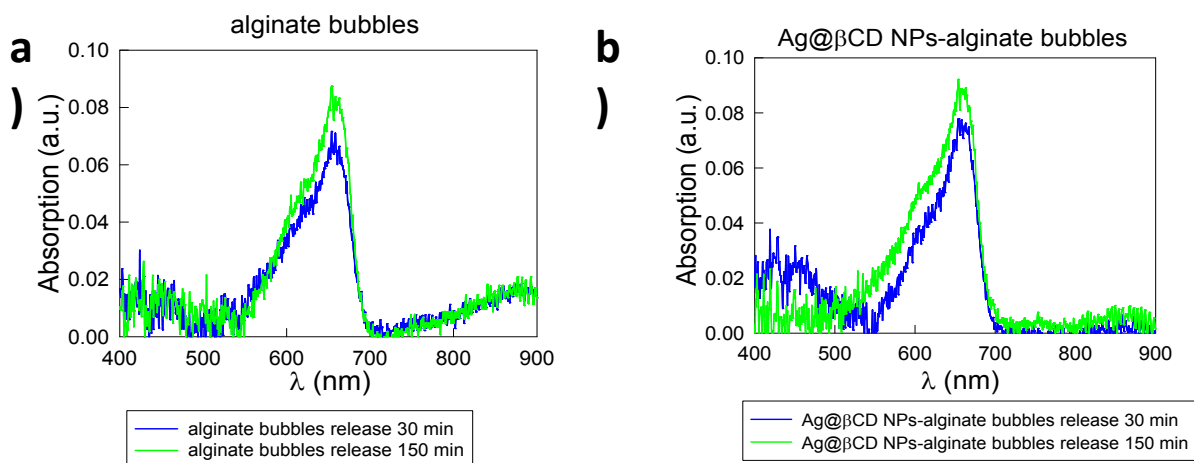


**Figure S5.** Release of entrapped MB. a) UV-vis spectrum of the water solution in which MB-loaded alginate bubbles are re-suspended after 30 min (blue) and 150 min (green) of soaking; b) UV-vis spectrum of the water solution in which MB-loaded Ag@βCD NPs-alginate bubbles are re-suspended after 30 min (blue) and 150 min (green) of soaking.

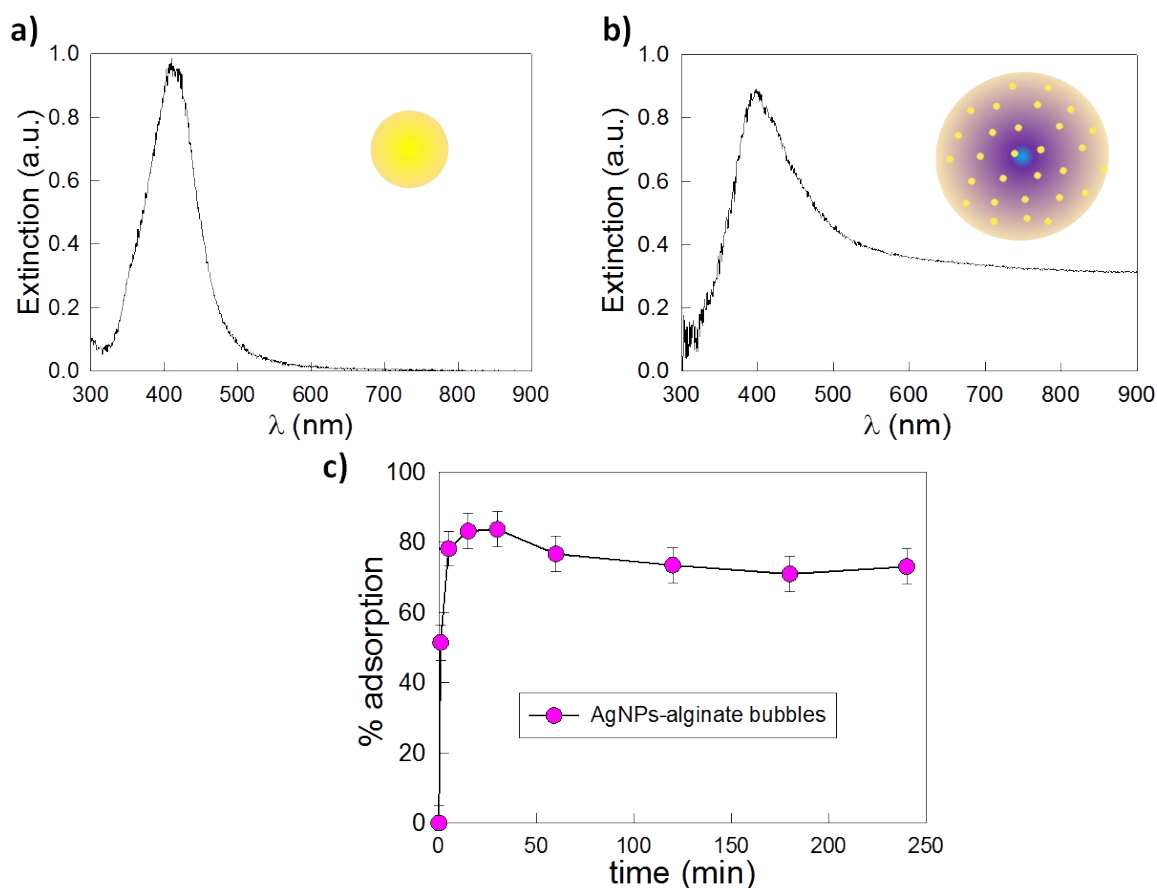


**Figure S6.** Characterization of non-functionalized Ag NPs systems. a) UV-Vis extinction spectrum of non-functionalized Ag NPs; b) UV-Vis extinction spectrum of Ag NPs-alginate hydrogel bubbles; c) % of adsorbed MB by Ag NPs-alginate hydrogel bubbles from aqueous solution ( $10^{-5}$  M) as a function of soaking time.

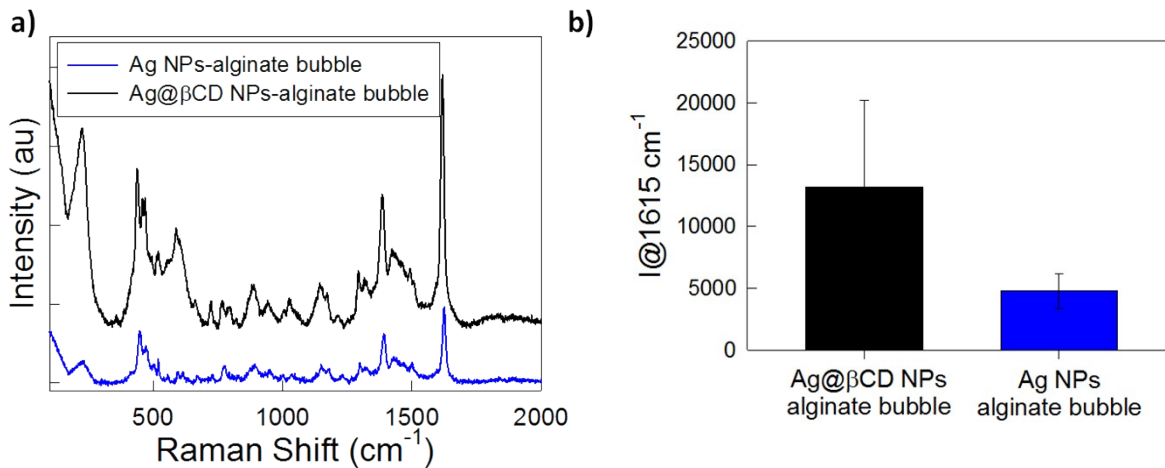


**Figure S7.** a) Comparison between the Raman spectra obtained using as absorbing and SERS substrate Ag@βCD NPs-alginate bubbles (black) and non-functionalized Ag NPs-alginate bubbles (blue) with 10<sup>-7</sup> M MB solution; b) comparison between the intensities of the Raman peak at 1615 cm<sup>-1</sup> of MB (10<sup>-7</sup>M) obtained from either Ag@βCD NPs-alginate or Ag NPs-alginate dried bubbles. Acquisition time 10s.

### SI 8. Intra-bubble Raman intensity variability

For the microRaman analysis, at least 6 different points were measured per each Ag@βCD-alginate bubble. The optical microscope coupled to the Raman instrument allows differentiating areas on the basis of morphology (crystals or dark spots) or colour (from white, to bright purple, light blue or black), indicating the presence inside the alginate matrix of NPs aggregates of different extents (**Figure S8a**). Different areas give rise to MB Raman signals with different intensities (**Figure S8b**), but the standard deviation calculated for the 1615 cm<sup>-1</sup> peak is about 10% (which is lower than the most of metallic SERS substrates).

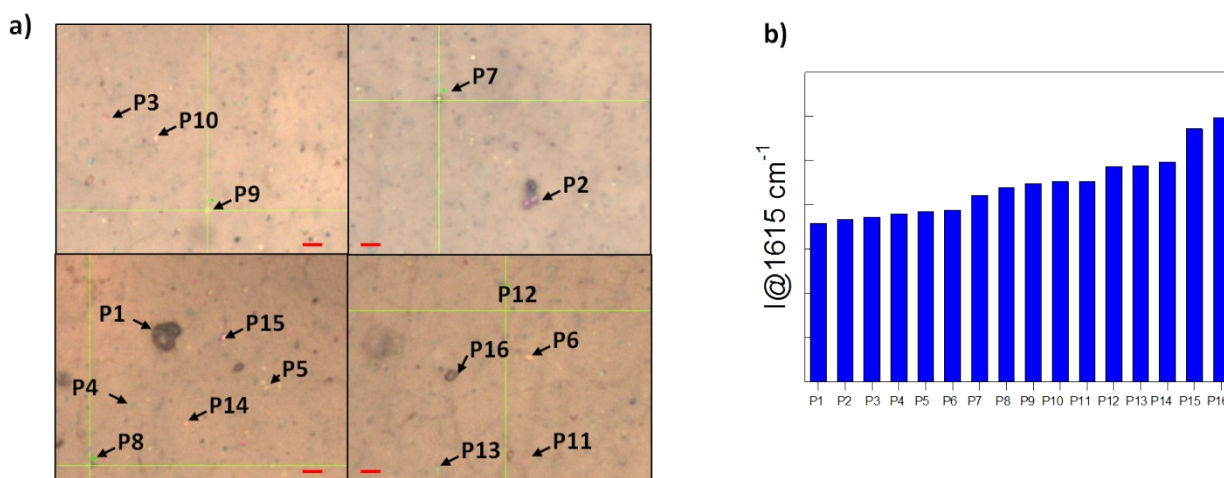


**Figure S8.** Intra-bubble Raman intensity variability. a) Optical images of the 16 different points of one dried Ag@βCD NPs-alginate bubble on which has been performed the microRaman

measurements (red bar: 5  $\mu\text{m}$ ); **b**) intensities of the Raman peak at 1615  $\text{cm}^{-1}$  of MB ( $10^{-7}\text{M}$ ) obtained from 16 different points of one dried Ag@ $\beta\text{CD}$  NPs alginate bubble. Acquisition time 1s.

### SI 9. Inter-bubble Raman intensity variability

Inter-bubble variability has been evaluated from  $\mu$ -Raman measurements on 6 different Ag@ $\beta\text{CD}$  NPs-alginate dried bubbles (each one measured in 6 different points) immersed in the same  $10^{-7}\text{M}$  MB solution. In the case of non-functionalized Ag NPs, measurements on 6 different dried bubbles (each one measured in 6 different points) have been performed after their immersion for 30 min in the same  $10^{-5}\text{M}$  MB solution. It is clearly visible that in both the cases there is a plasmonic bubble for which the medium Raman signal at 1615  $\text{cm}^{-1}$  is significantly higher than the others. Probably, most of the analyte is adsorbed by a limited number of the bubbles and in one of these the pre-concentration is remarkably higher than in the others. We ascribed this effect to the high rate of the adsorption process and to a different absorption capability of different bubbles, rather than different SERS behaviour. As visible from SI S8, even if it is possible to recognise areas with different NPs aggregates inside one plasmonic bubble, this fact does not cause high variability of Raman intensities. In addition, the presence of  $\beta\text{CD}$  on AgNPs surface seems not to be a crucial aspect for the determination of inter-bubble variability and this fact is a further hint suggesting that these differences are related to the adsorption process, rather than to the SERS mechanism.

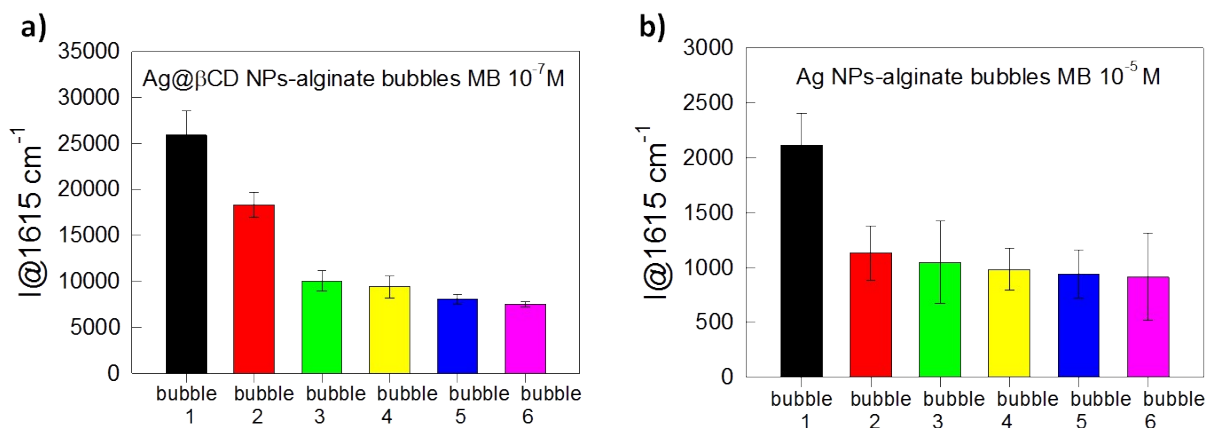


**Figure S9.** Inter-bubble Raman intensity variability Comparison between the intensities of the Raman peak at 1615  $\text{cm}^{-1}$  of **a**) MB ( $10^{-7}\text{M}$ ) obtained from 6 different dried Ag@ $\beta\text{CD}$  NPs- alginate bubbles simultaneously soaked in the same MB solution; **b**) MB ( $10^{-5}\text{M}$ ) obtained from 6 different dried Ag NPs- alginate bubbles simultaneously soaked in the same MB solution. Acquisition time 1s.

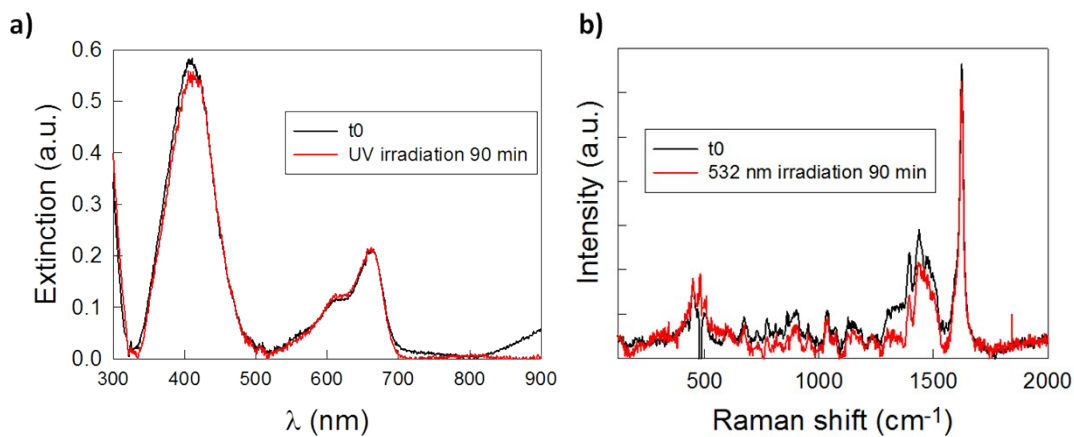


**Figure S10.** Photochemical stability of MB adsorbed on Ag@ $\beta$ CD NPs-alginate bubbles during 90 minutes of UV and visible illumination. **a)** UV-vis spectra of MB-loaded Ag@ $\beta$ CD NPs-alginate bubbles before (black) and after (red) 90 min of illumination with a UV lamp; **b)** Raman spectra of non-dried MB-loaded Ag@ $\beta$ CD NPs-alginate bubbles before (black) and after (red) 90 min of illumination with a 532 nm laser.